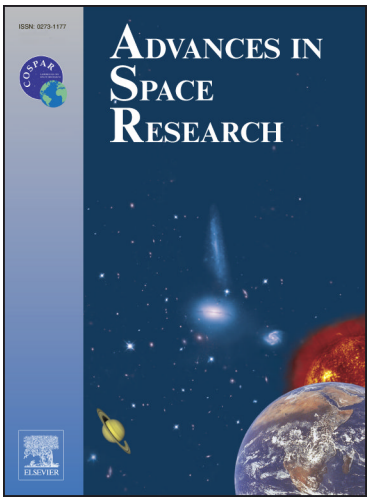

The Adjusted Optical Properties for Galileo/BeiDou-2/QZS-1 Satellites and Initial Results on BeiDou-3e and QZS-2 satellites

Bingbing Duan, Urs Hugentobler, Inga Selmke

PII: S0273-1177(18)30861-5
DOI: https://doi.org/10.1016/j.asr.2018.11.007
Reference: JASR 14012

To appear in: *Advances in Space Research*

Received Date: 29 July 2018
Accepted Date: 12 November 2018

Please cite this article as: Duan, B., Hugentobler, U., Selmke, I., The Adjusted Optical Properties for Galileo/ BeiDou-2/QZS-1 Satellites and Initial Results on BeiDou-3e and QZS-2 satellites, *Advances in Space Research* (2018), doi: https://doi.org/10.1016/j.asr.2018.11.007

The Adjusted Optical Properties for Galileo/BeiDou-2/QZS-1 Satellites and Initial Results on BeiDou-3e and QZS-2 satellites

Bingbing Duan, Urs Hugentobler, Inga Selmke

Institute for Astronomical and Physical Geodesy, Technical University of Munich, Arcisstr 21, 80333, Munich, Germany

Abstract

Solar Radiation Pressure (SRP) is the dominant non-gravitational perturbation for GNSS (Global Navigation Satellite System) satellites. In the absence of precise surface models, the Empirical CODE Orbit Models (ECOM, ECOM2) are widely used in GNSS satellite orbit determination. Based on previous studies, the use of an a priori box-wing model enhances the ECOM model, especially if the spacecraft is a stretched body satellite. However, so far not all the GNSS system providers have published their metadata. To ensure a precise use of the a priori box-wing model, we estimate the optical parameters of all the Galileo, BeiDou-2, and QZS-1 (Quasi Zenith Satellite System) satellites based on the physical processes from SRP to acceleration. Validation using orbit prediction proves that the adjusted parameters of Galileo and QZS-1 satellites exhibit almost the same performance as the corresponding published and "best guess" values. Whereas, the estimated parameters of BeiDou-2 satellites demonstrate an improvement of more than 60% over the initial "guess" values. The resulting optical parameters of all the satellites are introduced into an a priori box-wing model, which is jointly used with ECOM and ECOM2 model in the orbit determination. Results show that the pure ECOM2 model exhibits better performance than the pure ECOM model for Galileo, BeiDou-2 GEO and QZS-1 orbits. Combined with the a priori box-wing model the ECOM model (ECOM+BW) results in the best Galileo, BeiDou-2 GEO and QZS-1 orbits. The standard deviation (STD) of satellite laser ranging residuals reduce by about 20% and 5% with respect to the pure ECOM2 model for Galileo and BeiDou-2 GEO orbits, while the reductions are about 40% and 60% for QZS-1 orbits in yaw-steering and orbit-normal mode respectively. BeiDou-2 IGSO and MEO satellite orbits do not benefit much from the a priori box-wing model. In summary, we suggest setting up a unified SRP model of ECOM+BW for Galileo, QZS-1, and BeiDou-2 orbits based on the adjusted metadata. In addition, we estimate the optical parameters of BeiDou-3e and QZS-2 satellites using a limited number of tracking stations. Results regarding the unified SRP model indicate the same advantages, the STD of satellite laser ranging residuals reduces by about 30% and 20% for QZS-2 and BeiDou-3e orbits respectively over orbit products without a priori model. The estimation procedure is effective and easy to apply to the new emerging satellites in the future.

Keywords: Solar radiation pressure model, Optical property adjustment, Box-wing model, Metadata, QZS-2 and BeiDou-3e

1. Introduction

Over the past few years, European Galileo navigation satellite system, Chinese BeiDou satellite navigation system (BDS, denotes BeiDou-2 in this study), and Japanese QZSS have all experienced fast development. Since the launches of the first In Orbit Validation Element (GIOVE) satellite in 2005 a total number of 22 Galileo satellites including Full Operational Capability (FOC) satellites are available until the middle of 2018. BDS consists of three types of constellations: Geostationary Orbit (GEO), Inclined Geosynchronous Orbit (IGSO), and Medium Earth Orbit (MEO) satellites. The initial generation BeiDou-2 has formed a space segment of 5 GEO satellites, 5 IGSO satellites, and 4 MEO satellites (Guo et al., 2016). By evaluating the performance of BeiDou-3 experimental (BeiDou-3e, 2 IGSO and 3 MEO) satellites, the next generation BeiDou-3 is proposed to aggregate 3 GEO satellites, 3 IGSO satellites and 24 MEO satellites (Zhao et al., 2018b). QZSS is a regional navigation satellite system developed by Japan Aerospace Exploration Agency (JAXA) to enhance the quality of GNSS applications in the Asia-Pacific region (Inaba et al., 2009). With the launches of QZS-4 in October 2017, there are now 4 QZSS satellites (QZS-1, QZS-2, QZS-3, QZS-4) in orbit. As stated by NSPCJ (National Space Policy Secretariat of Japan, http://qzss.go.jp), QZS-3 is a GEO satellite while the others are IGSO satellites.

To enhance the service of Multi-GNSS, the IGS (International GNSS Service) initiated the MGEX (Multi-GNSS Experiment) in August 2011. Over the more than 5 years

Email addresses: bingbing.duan@tum.de (Bingbing Duan), urs.hugentobler@bv.tum.de (Urs Hugentobler), inga.selmke@tum.de (Inga Selmke)

of its development the MGEX has comprised 6 data analysis centers (ACs) and has recruited a large number of Multi-GNSS tracking stations. Montenbruck et al. (2017b) summarized the achievements of the precise GNSS orbits by a cross-comparison between individual MGEX ACs over half a year in 2016. 3D RMSs are about 3 to 6 cm for GPS, 6 to 17 cm for GLONASS, 16 to 29 cm for Galileo IOV, 14 to 26 cm for Galileo FOC, 510 cm for BDS GEO, 32 to 51 cm for BDS IGSO, 12 to 26 cm for BDS MEO, 40 to 73 cm for QZSS YS (Yaw-Steering) mode, and 123 to 240 cm for QZSS ON (Orbit-Normal) mode. Obviously, the RMS values of Galileo, BDS and QZSS orbits are not as good as for GPS and GLONASS orbits. The sparse and non-globally distributed tracking stations on one hand prevent the calculation from good geometry and sufficient observations. On the other hand, the imperfect SRP model also limits the quality of the orbit products.

Following Fliegel et al. (1992); Fliegel and Gallini (1996) accelerations aroused by SRP for a GNSS satellite depend mainly on its dimension, optical property, mass, and attitude. Unlike Galileo satellites, BDS system operators have so far not yet published all their metadata. QZSS system providers published all the metadata in the middle of 2018 except the optical parameters of QZS-1 satellite. Without a priori knowledge, the ECOM and ECOM2 models (Beutler et al., 1994; Arnold et al., 2015) are widely used by most of the MGEX ACs (Deng et al., 2016; Li et al., 2015; Steigenberger et al., 2015a). Prange et al. (2017) verified that there was a clear improvement for Galileo and QZS-1 orbits by using the ECOM2 model over the ECOM model, but a slight degradation was found for BDS IGSO and BDS MEO orbits.

To make use of a satellite metadata, Rodriguez-Solano et al. (2012a) developed an adjustable box-wing model for GPS satellites and got comparable results as the ECOM model. Steigenberger et al. (2015b) set up a simple a priori box-wing model for Galileo GIOVE-B satellite and found that the periodical orbit and clock errors reduced significantly. Zhao et al. (2018a) proved that an a priori box-wing model improved the accuracy of QZS-1 orbits significantly when the satellite was in ON mode. Montenbruck et al. (2015b) introduced an enhanced approach of modeling isolating the impact of asymmetric and symmetric contributions of satellite surfaces. The peak magnitude of radial orbit errors for Galileo satellites reduced from 20 cm to 5 cm. Following that, the model was extended to QZS-1 satellite as a semi-analytical SRP modeling considering the ON mode as well (Montenbruck et al., 2017a). The new QZS-1 orbits marked a 2-4 times improvement over the previous orbit products without a priori model.

Guo et al. (2017) suggested adding a tightly constrained acceleration in the along-track component for BDS IGSO and MEO satellites and concluded that the orbit overlap errors improved by roughly a factor of eight during ON mode. Zhao et al. (2018b) presented initial results of BeiDou-3e satellite orbits involving details on satellite yaw attitude, Phase Center Offset (PCO), and signal frequencies. Following that, Wang et al. (2018) did initial tests on SRP models for BeiDou-3e orbits, where a slightly better result was identified when applying an a priori box-wing model based on the "guess" metadata.

Based on this background, we estimate the optical properties of all the Galileo, BeiDou-2 and QZS-1 satellites to involve more accurate box-wing parameters into the a priori box-wing model. Following that, we test four types of SRP models for all the constellations by using ECOM and ECOM2 models as well as their combination with the a priori box-wing model. Finally, initial results on BeiDou-3e and QZS-2 satellites are presented as well.

2. SRP Acceleration

The physical optical properties of a satellite surface comprises absorbed (α), reflected (ρ) and diffusely (δ) scattered photons. Milani et al. (1987) formulated the physical interaction between SRP and accelerations in the following way

$$\boldsymbol{f} = -\frac{A}{M}\frac{S_0}{c} cos\theta \left[(\alpha+\delta)\boldsymbol{e}_D + 2(\frac{\delta}{3} + \rho\cos\theta)\boldsymbol{e}_N) \right] \quad (1)$$

where A denotes the surface area, M the total mass of satellite, S_0 the solar flux at 1 AU, c the vacuum velocity of light. Furthermore, $\boldsymbol{e}_D$ denotes the unit vector in Sun direction, $\boldsymbol{e}_N$ the normal vector of the satellite surface, and θ the angle between both vectors. In case of satellite surface covered by multi-layer insulation (MLI), the energy absorbed by the satellite surface is considered to be instantaneously re-radiated back into the space according to Lambert's law

$$\boldsymbol{f} = -\frac{A}{M}\frac{S_0}{c} cos\theta \left[(\alpha+\delta)(\boldsymbol{e}_D + \frac{2}{3}\boldsymbol{e}_N) + 2\rho\cos\theta\boldsymbol{e}_N \right] \quad (2)$$

(Rodriguez-Solano et al., 2012a). For the solar panel, we assume that temperatures for the front and back sides are the same, and the thermal re-emission is mostly balanced. There is also an implicit condition in equation (2) that $\alpha+\delta+\rho = 1$. Thus, the SRP acceleration depends mainly on the satellite attitude and metadata information.

2.1. Satellite Attitudes

The current GNSS satellites use YS or ON attitude control strategy or the combination of these two. The YS mode is defined by three unit vectors

$$\begin{aligned} \boldsymbol{e}_{z,YS} &= -\frac{\boldsymbol{r}}{|r|} \\ \boldsymbol{e}_{y,YS} &= \frac{\boldsymbol{e}_D \times \boldsymbol{r}}{|\boldsymbol{e}_D \times \boldsymbol{r}|} \\ \boldsymbol{e}_{x,YS} &= \boldsymbol{e}_{y,YS} \times \boldsymbol{e}_{z,YS} \end{aligned} \quad (3)$$

where $\boldsymbol{r}$ is the geocentric satellite position vector. The vector $\boldsymbol{e}_{z,YS}$ points toward the center of the Earth, $\boldsymbol{e}_{y,YS}$ is perpendicular to the Sun and nadir direction, and $\boldsymbol{e}_{x,YS}$

completes the right handed frame with the positive direction pointing toward the sun-lit hemisphere. Whereas, the ON mode defines the reference orientation of a spacecraft aligned with the orbital frame by three unit vectors

$$\begin{aligned} \boldsymbol{e}_{z,ON} &= -\frac{\boldsymbol{r}}{|r|} \\ \boldsymbol{e}_{y,ON} &= \frac{\boldsymbol{r} \times \boldsymbol{v}}{|\boldsymbol{r} \times \boldsymbol{v}|} \\ \boldsymbol{e}_{x,ON} &= \boldsymbol{e}_{y,ON} \times \boldsymbol{e}_{z,ON} \end{aligned} \tag{4}$$

where $\boldsymbol{v}$ is the inertial velocity of a satellite. Accordingly, $\boldsymbol{e}_{z,ON}$ points to the center of the Earth, $\boldsymbol{e}_{y,ON}$ is perpendicular to the orbital plane, and $\boldsymbol{e}_{x,ON}$ is roughly oriented in anti-flight direction.

Galileo satellites take YS mode, BDS GEO satellites maintain ON mode, BDS IGSO, BDS MEO and QZS-1 satellites take two different attitude modes depending on the elevation of the Sun above the orbital plane (β). When $|\beta| \geq 4°$ BDS IGSO and BDS MEO satellites maintain nominal YS mode, and switch to ON mode in case of $|\beta| < 4°$ (Dai et al., 2015). Ishijima et al. (2009) introduced that QZS-1 used a YS attitude for most of its mission and switched to ON mode when $|\beta| \leq 20°$. Despite taking the same YS mode, directions of individual axes in the satellite body frame are not identical for Galileo, BDS, and QZS-1. Montenbruck et al. (2015a) describe that +x axis of Galileo and QZSS satellites are oriented away from the Sun while that of BDS is pointed toward the sun-lit hemisphere. However, the IGS defines that +x-axis of all the Galileo, BDS and QZSS satellites is always pointing towards the sun-lit hemisphere. Thus, for consistency with IGS the following discussions regarding the direction of satellite body frame in this study always refer to the IGS definition.

2.2. The Initial Metadata for Box-wing Model

The European GNSS service center (https://www.gsc-europa.eu) has published the detailed metadata of Galileo IOV and FOC satellites since 2017. Montenbruck et al. (2017a) presented the approximate body dimensions as well as the "best guess" optical properties of QZS-1 satellite, and proved that the "best guess" values fitted the results fairly well except for the y-panel due to some unclear reasons related to the radiators. Guo et al. (2016) presented the approximate dimensions and the overall optical properties of BeiDou-2 satellites. In general, for each of the satellite surfaces there is probably more than one type of material. For the convenient use of the metadata, we integrate the optical properties of all the materials of the same surface according to the proportion of the area. The combined initial metadata of Galileo, BDS, and QZS-1 satellites are shown in Table 1, in which "sp" denotes the front side of solar panel.

In fact, in October 2017 NSPCJ published the dimensions of QZS-1 (as shown in Table 3), but declared that the optical properties were still under investigation. Thus, in our adjustment, dimensions of Galileo and QZS-1 satellites are fixed to the officially published values, while BDS satellites are prepared with the approximate values. The surface optical properties in Table 1 are taken as initial "a priori" values in the least square adjustment. The total mass of a satellite is taken from the IGS MGEX suggestions (http://mgex.igs.org), as shown in Table 2.

3. Adjustment of Optical Properties

In this section, equation (2) is applied in our box-wing model to study the properties of all the six body surfaces, while equation (1) is adopted for the solar panel. For each satellite surface there are two adjusted optical parameters: $\alpha + \delta$ and ρ. The respective partial derivatives can be written as follows

$$\frac{\boldsymbol{f}}{\partial(\alpha+\delta)} = -\frac{A}{M}\frac{S_0}{c} cos\theta(\boldsymbol{e}_D + \frac{2}{3}\boldsymbol{e}_N) \tag{5}$$

$$\frac{\boldsymbol{f}}{\partial(\rho)} = -\frac{A}{M}\frac{S_0}{c} \cdot 2cos^2\theta \boldsymbol{e}_N \tag{6}$$

In YS mode, there are 6 optical parameters corresponding to +x and ±z surfaces. To compensate the direct radiation as well as the misalignment of solar panels, a constant parameter in Sun-satellite direction ($\boldsymbol{e}_D$), y-bias, and a rotation lag of solar panel are adopted as well. In ON mode, the solar panel effect cannot be compensated very well by an acceleration in the $\boldsymbol{e}_D$ direction, and ±y surfaces contribute also to the SRP accelerations. Hence, in ON mode we estimate optical properties of all the satellite surfaces as well as the optical property ρ of the solar panel while assuming that optical properties in the top and bottom sides of x and y panels are identical.

We use observations of about 80 tracking stations (Figure 1) over half a year (2017 day 180 to 2017 day 365) from the TUM (Technical University of Munich) AC. For details of 2-step orbit determination approach we can refer to Steigenberger et al. (2013, 2015a); Selmke and Hugentobler (2017). The Bernese GNSS Software (Dach et al., 2007) is employed in a special version modified to support the estimation of optical properties as well as empirical parameters. Days with maneuvers are excluded from the analysis. Observations within the eclipses are not considered. The relevant conventions and processing standards are summarized in Table 3. The observation types C1I and C2I of BDS both stand for the frequency of B1, stations providing either type are included in our estimation. SRP parameter lag in Table 3 denotes the solar panel rotation lag, Y_0 the y-bias, SP the direct radiation pressure, ±XAD ±x surface $\alpha + \delta$, ±XR ±x surface ρ, ±ZAD ±z surface $\alpha + \delta$, ±ZR ±z surface ρ, SPR solar panel ρ.

3.1. Correlations between Parameters

Optical parameters are adjusted every daily arc without any constraints, the correlation coefficients between

Table 1: The combined initial metadata of Galileo IOV, Galileo FOC, BeiDou-2, and QZS-1 satellites

IOV	$A(m^2)$	α	ρ	δ	FOC	$A(m^2)$	α	ρ	δ
+x	1.320	0.940	0.000	0.060	+x	1.320	0.930	0.000	0.070
−x	1.320	0.444	0.435	0.131	−x	1.320	0.363	0.487	0.150
+y	3.000	0.388	0.473	0.139	+y	2.783	0.425	0.434	0.141
−y	3.000	0.380	0.480	0.140	−y	2.783	0.460	0.404	0.136
+z	3.000	0.782	0.094	0.124	+z	3.022	0.695	0.143	0.161
−z	3.000	0.940	0.000	0.060	−z	3.022	0.661	0.231	0.108
sp	10.820	0.914	0.086	0.000	sp	10.820	0.914	0.086	0.000
BeiDou-2	$A(m^2)$	α	ρ	δ	QZS-1	$A(m^2)$	α	ρ	δ
+x	3.748	0.350	0.650	0.000	+x	12.200	0.846	0.019	0.135
−x	3.748	0.350	0.650	0.000	−x	12.200	0.846	0.019	0.135
+y	4.400	0.114	0.856	0.000	+y	12.600	0.547	0.327	0.126
−y	4.400	0.114	0.856	0.000	−y	12.600	0.463	0.417	0.120
+z	3.440	0.350	0.650	0.000	+z	6.000	0.607	0.067	0.327
−z	3.440	0.350	0.650	0.000	−z	6.000	0.940	0.000	0.060
sp	22.704	0.720	0.280	0.000	sp	40.000	0.750	0.210	0.040

Table 2: Total mass of satellite in the adjustment, unit(kg)

PRN	Mass	PRN	Mass	PRN	Mass
E01	706.7	E11	696.8	E30	707.7
E02	707.6	E12	695.3	BeiDou-2	2200.0
E03	709.9	E14	662.1	C31	848.0
E04	708.8	E18	661.0	C32,C33,C34	2800.0
E05	709.8	E19	697.6	C35	1000.0
E07	706.6	E22	705.9	J01	2281.0
E08	709.1	E24	708.8	J02	2324.2
E09	707.9	E26	705.7	-	

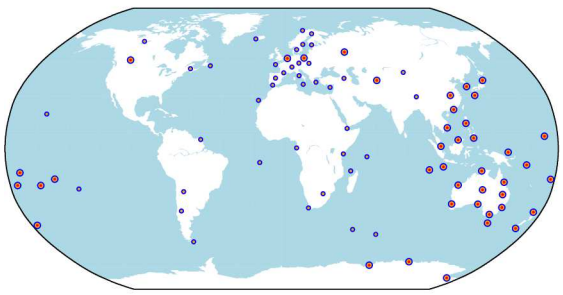

Figure 1: Tracking network, all the stations track Galileo and BDS observations, 41 stations track QZS-1 observations (big circles)

Table 3: Modeling options for optical property adjustment

Items	Value
Galileo obs types	C1C/C1X,C5Q/C5X,L1C/L1X, L5Q/L5X
QZSS obs types	C1C/C1X,C2X,L1C/L1X,L2X
BDS obs types	C2I/C1I,C7I,L2I/L1I,L7I
Observations	Undifferenced ionosphere-free code and phase combination
Data arc	1 day
Sampling	5 min
Elevation cutoff	5°
PCO and variations	IGS14 ANTEX
SRP parameters	YS:lag,Y_0,SP,+XAD,+XR, +ZAD,+ZR,−ZAD,−ZR ON:SPR,±XAD,±XR,±YAD, ±YR,+ZAD,+ZR,−ZAD,−ZR
Earth albedo	Considered (Rodriguez-Solano et al., 2012b)
Antenna thrust	Not considered
Station coordinate	Fixed on GPS precise point positioning (PPP)
Troposphere delay	Fixed on GPS PPP
Receiver clock	Fixed on GPS PPP
Satellite clock	Estimated
Receiver system bias	Estimated

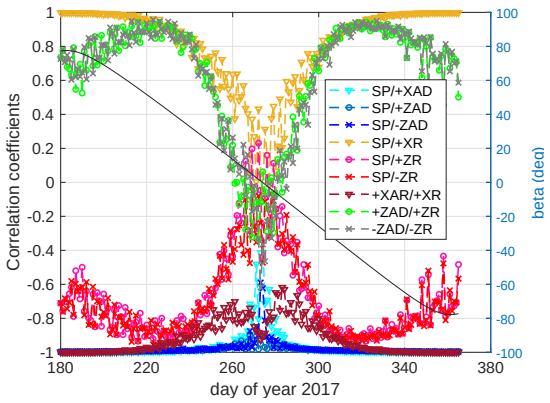

Figure 2: Correlation coefficients between unconstrained parameters in YS mode by combining 3 days' normal equations (the β angle is indicated by a solid black line)

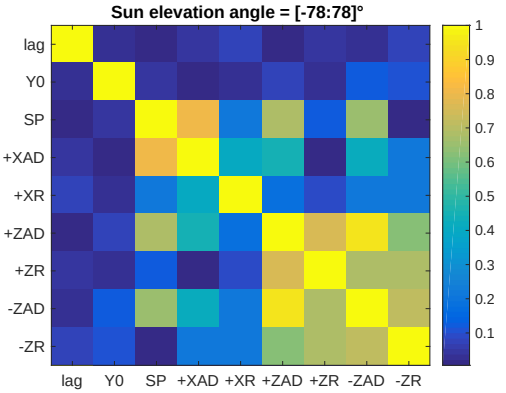

Figure 3: Absolute values of correlation coefficients between unconstrained parameters in YS mode after stacking all the normal equations

unconstrained parameters in YS mode by combining every 3 days' normal equations are shown in Figure 2. There is a clear dependency of the correlation coefficients on the β angle. In particular, the absorption plus diffusion terms (AD) are highly correlated with respect to SP parameter when the absolute value of β angle is larger than 20°. Thus, it is not possible to obtain accurate optical parameters from only one or several daily solutions.

Beutler et al. (1996) combined consecutive short arcs into long arcs for precise GPS orbit determination. Following the same procedure, we stack all the daily normal equations of half a year after pre-eliminating all parameters except the optical parameters. Figure 3 shows the absolute values of correlation coefficients between all the unconstrained parameters after stacking of all the daily normal equations. The correlations do not vanish but most of them are not significant, and we find that the formal errors of all the parameter are reasonably small. However, correlations between parameters in ON mode are much higher than in YS mode due to the small range of β angle. Results of BDS GEO satellites demonstrate that formal errors of parameters for the x-panel after stacking all the normal equations are two times larger than those in YS mode, while those for the y-panel are ten times worse. Hence, parameters for x-panel and y-panel are constrained for the processing of GEO satellites. For QZS-1, BDS IGSO, and BDS MEO satellites, we firstly estimate the YS mode parameters, and subsequently, observations in ON mode are used to adjust $\pm$y surface parameters as well as the solar panel ρ while fixing all the parameters on values determined in YS mode.

3.2. Results from Adjustment

The adjusted parameters of Galileo, QZS-1, and BDS satellites are discussed one after the other. We compare the estimated corrections to the initial values, check the formal errors of all the parameters, and evaluate whether the summed values of optical properties are equal to 1. The top part of Figure 4 shows the averaged results of all the Galileo IOV and FOC satellites respectively. Galileo satellites are constantly in YS mode, estimations for +x- and $\pm$z-panels are all close to the published values, all the formal errors are smaller than 0.025, and furthermore, the summed values of optical properties are all very close to 1 for each surface. The results demonstrate that our estimation procedure reproduces the published Galileo metadata fairly well. Moreover, indicated by equation (1), the adopted dimensions and masses of Galileo satellites in our estimation all prove to be close to the true values. QZS-1 satellite takes both YS and ON modes, the adjusted parameters (Figure 4 bottom) do not agree very well with the initial values, but all the formal errors are reasonably small. The +z-surface carries the GNSS antenna and consequently the estimations are different from the $-$z-parameters. However, the sums of $\alpha + \delta$ and ρ are almost the same for the $\pm$z-panels, which indicates an identical scaling factor for $\alpha+\delta+\rho$. So, the deviation of the summed values from 1 for the $\pm$z-panels might be due to errors in the dimensions or the total mass of the satellite. However, the summed values of parameters related to the y-panel deviate too much from 1, which is potentially caused by radiators on the y-panel.

BDS IGSO and MEO satellites take also both YS and ON modes, optical properties are assumed to be the same for all the available satellites. The top part of Figure 5 illustrates the averaged results of all the BDS IGSO and MEO satellites. The estimations deviate from the initial values despite having small formal errors. The summed values of all the surfaces are close to 1 except for +z. Unlike the QZS-1 satellite, the summed values of parameters in $\pm$z-panels are not close to each other due to some unknown reasons, probably optical properties in $\pm$z-panels are not identical for all the BDS IGSO and MEO satellites. For BDS GEO satellites, we need to mention that the +x-panel holds the C-band telecommunication antenna, which seems to be as large as the x-panel. To accommodate the effect of that, we consider the C-band antenna to

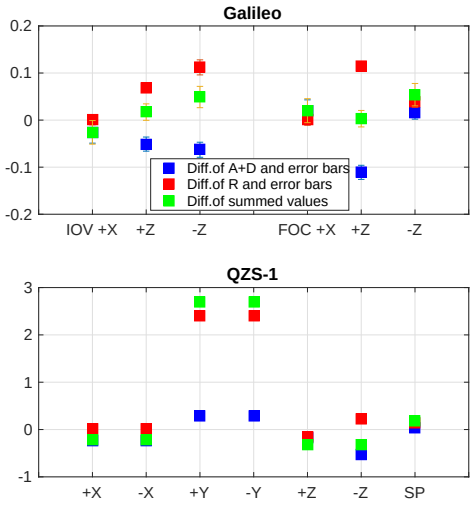

Figure 4: Evaluation of adjusted metadata for Galileo (IOV, FOC) and QZS-1 satellites. The blue color represents the difference between adjusted $\alpha+\delta$ and the initial values, the red color denotes the difference between adjusted ρ and the initial values, the green color means the deviation of the summed values from 1.

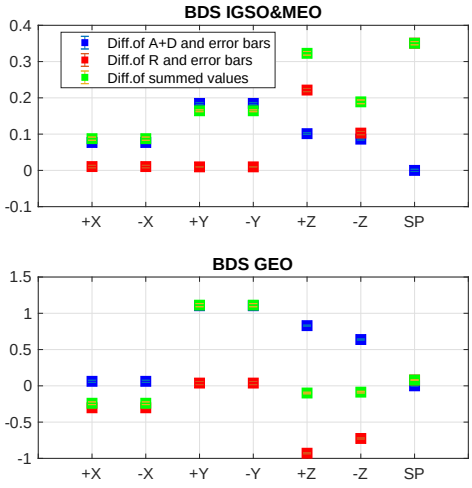

Figure 5: Evaluation of adjusted metadata for BDS IGSO, BDS MEO and GEO satellites. The blue color represents the difference between adjusted $\alpha+\delta$ and the initial values, the red color denotes the difference between adjusted ρ and the initial values, the green color means the deviation of the summed values from 1.

be part of the z-panel according to the figures in MGEX (http://mgex.igs.org), and an area of 4 square meters is accordingly added to the z-panel. Besides, we find that it is better to process BDS GEO satellites together with BDS IGSO and MEO satellites in order to estimate precise receiver system biases. Results verify that the joint adjustment reduces the day boundary discontinuities in along-track component by a factor of ten compared to dealing with only GEO satellites. The bottom part of Figure 5 shows that the estimations of BDS GEO satellites deviate from the initial values, all the formal errors are reasonably small after adding a constraint of 0.01 on the x- and y-panel parameters. The deviation of the summed values from 1 for the y-panel are larger than 1 due to the small range of β angle as well as the unknown details on radiators. The summed values of parameters for the $\pm$z-panels are both very close to 1, which indicates that the additionally added area is reasonable.

All the estimated parameters are given in Table 4. As discussed above, parameters for the y-panel are not well adjusted in ON mode, optical properties of greater than 1 exist in an unphysical manner. $\pm$z-parameters in both YS and ON modes are not constrained in the adjustment, the systematic errors might contaminate the estimations since $\alpha+\delta$ and ρ are correlated. The adjusted parameters of $\pm$z-panels for BDS GEO satellites exhibit that $\alpha+\delta$ properties are greater than 1 and ρ properties are smaller than 0, however, the sums of $\alpha+\delta$ and ρ are close to 1. Thus, the SRP accelerations are mostly balanced.

3.3. Validation of Orbit Prediction

To evaluate whether the adjusted parameters are reasonable, we firstly fit the precise gbm orbits from the GFZ

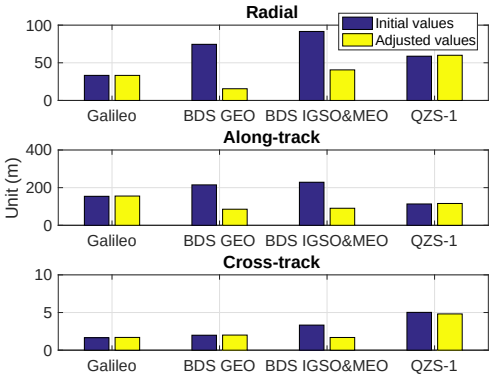

Figure 6: The averaged RMS of predicted orbits for all the satellites based on the initial (blue) and the adjusted (yellow) optical properties respectively.

(German Research Center for Geosciences) AC of one day to generate a precise initial condition. Then, an orbit arc length of 7 days is predicted using the box-wing model. Finally, predictions with the initial (values in Table 1) and the estimated parameters are compared to the precise gbm orbits. Eclipsing satellites are excluded from the comparison. Figure 6 illustrates the averaged RMS of differences of the predicted orbits based on the initial (blue) and the adjusted metadata (yellow) respectively. Galileo and QZS-1 satellites perform almost the same in the two cases, while BDS orbit predictions exhibit a large improvement of more than 60% by using the adjusted parameters. In summary, we suggest using either the initial metadata or the adjusted parameters for Galileo and QZS-1 satellites, but using the adjusted optical properties for BDS based on the approximate dimensions. Meanwhile, BDS system operators are

Table 4: The estimated optical properties and formal errors for Galileo (IOV, FOC), BDS GEO, BDS IGSO and MEO (BDS I&M), and QZS-1 satellites

Galileo	$A(m^2)$	$\alpha+\delta$	ρ	QZS-1	$A(m^2)$	$\alpha+\delta$	ρ
IOV +x	1.320	0.974±0.023	0.000±0.010	+x	13.395	0.749±0.015	0.040±0.006
IOV +z	3.000	0.855±0.015	0.162±0.009	−x	13.395	0.749±0.015	0.040±0.006
IOV −z	3.000	0.877±0.016	0.172±0.016	+y	13.395	0.967±0.006	2.722±0.032
FOC +x	1.320	1.020±0.023	0.000±0.011	−y	13.395	0.967±0.006	2.722±0.032
FOC +z	3.022	0.745±0.015	0.258±0.009	+z	5.523	0.768±0.014	-0.082±0.012
FOC −z	3.022	0.785±0.014	0.269±0.011	−z	5.523	0.411±0.015	0.278±0.013
				sp	40.000	0.820±0.000	0.350±0.008
BDS GEO	$A(m^2)$	$\alpha+\delta$	ρ	BDS I&M	$A(m^2)$	$\alpha+\delta$	ρ
+x	3.748	0.412±0.014	0.347±0.011	+x	3.748	0.427±0.016	0.660±0.008
−x	3.748	0.412±0.014	0.347±0.011	−x	3.748	0.427±0.016	0.660±0.008
+y	4.400	1.218±0.002	0.894±0.017	+y	4.400	0.299±0.018	0.866±0.019
−y	4.400	1.218±0.002	0.894±0.017	−y	4.400	0.299±0.018	0.866±0.019
+z	7.440	1.180±0.007	-0.279±0.008	+z	3.440	0.451±0.016	0.871±0.008
−z	7.440	0.988±0.007	-0.076±0.008	−z	3.440	0.436±0.012	0.753±0.007
sp	22.704	0.720±0.000	0.360±0.002	sp	22.704	0.720±0.000	0.631±0.005

urged to make all the detailed metadata of their satellites available.

4. Optimal SRP Models and Orbit Validation

With the adjusted metadata, we test the performance of ECOM models and their combination with an a priori box-wing (BW) model in the following four cases.
- 5-parameter ECOM model
- 5-parameter ECOM+BW model
- 9-parameter ECOM2 model
- 9-parameter ECOM2+BW model

For the YS mode the empirical parameters are given in a Sun-oriented $\boldsymbol{DYB}$ frame with $\boldsymbol{D}$ pointing towards the Sun, $\boldsymbol{Y}$ along the solar axis, and $\boldsymbol{B}$ completing the right handed system. Because in ON mode the solar panel is not perpendicular to the Sun-satellite direction, a modified $\overline{\boldsymbol{DYB}}$ frame is used with $\overline{\boldsymbol{Y}}$ perpendicular to the orbital plane, $\overline{\boldsymbol{B}}$ perpendicular to $\overline{\boldsymbol{Y}}$ and the Sun-satellite direction, $\overline{\boldsymbol{D}}$ completing the right handed system pointing into the direction of the Sun's projection to the orbital plane. Tracking stations are the same as in section 3. All the settings but the SRP parameters in orbit determination are the same as in Table 3. Satellite laser ranging (SLR)(Pearlman et al., 2002) residuals are considered to evaluate the quality of the orbits.

All the Galileo satellites are constantly in YS mode, the averaged mean offsets and standard deviations (STDs) of SLR residuals are given in Table 5. Use of the pure ECOM2 model reduces the STD of the SLR residuals by about 30% over the pure ECOM model. Combined with an a priori box-wing model the ECOM model results in the best orbits and reduces the STD further by 20% over the pure ECOM2 model. There is very small change in the STD after adding the a priori box-wing model to the ECOM2 model, but the mean offset of the SLR residuals is clearly reduced.

Table 5: Averaged mean offsets and STDs of SLR residuals for all the Galileo orbits, unit (cm)

Solution	Mean	STD
ECOM	1.5	8.2
ECOM+BW	1.7	4.2
ECOM2	1.8	5.4
ECOM2+BW	0.9	5.2

SLR observations are not available for every BDS satellite. GEO satellite C01, IGSO satellites C08, C10, C13 and MEO satellites C11 have sufficient SLR observations during the experimental period and are thus employed to evaluate the quality of BDS GEO, IGSO and MEO orbits. Information for SLR residuals in YS and ON modes are shown in Table 6. The pure ECOM2 model exhibits better results than the the pure ECOM model for BDS GEO orbits while showing worse results for BDS IGSO and MEO orbits, especially during the ON mode. Combined with the a priori box-wing model the ECOM model reduce the STD of SLR residuals by about 15% over the pure ECOM model for BDS GEO orbits and the improvement of the mean offset is a factor of two. However, for BDS IGSO and MEO orbits the ECOM and ECOM2 models do not benefit much from the a priori box-wing model.

Figure 7 illustrates the SLR residuals of QZS-1 orbits for the four types of SRP models covering both YS mode and ON mode periods. The orbits without the a priori box-wing model exhibit a clear dependency of the SLR residuals on the β angle. Combined with the a priori box-wing model such β angle variations are notably reduced.

Table 6: Averaged mean offsets and STDs of SLR residuals for BeiDou-2 orbits, unit (cm)

Solution	BDS GEO		BDS IGSO		BDS MEO	
	YS	ON	YS	ON	YS	ON
ECOM	-	48.4±21.2	2.1±10.0	2.9±12.3	2.7±12.2	−3.0±16.4
ECOM+BW	-	23.4±17.7	2.7±10.8	4.4±12.3	5.6±13.1	7.4±17.4
ECOM2	-	32.4±18.3	4.7±14.1	6.9±15.9	6.7±15.3	4.2±20.0
ECOM2+BW	-	22.4±17.2	−10.8±16.4	−6.3±16.5	6.3±16.5	2.8±21.4

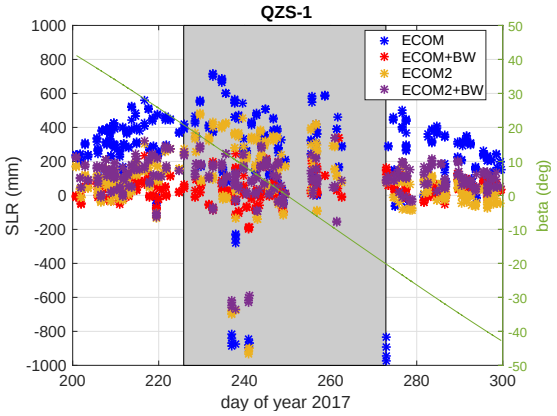

Figure 7: SLR residuals of QZS-1 orbits. (blue: pure ECOM, red: ECOM+BW, yellow: pure ECOM2, purple: ECOM2+BW). The β angle is indicated by a solid green line and the ON mode period is indicated in grey.

Table 7: Averaged mean offsets and STDs of SLR residuals for QZS-1 orbits, unit (cm)

Solution	YS		ON	
	Mean	STD	Mean	STD
ECOM	25.3	19.9	22.8	33.7
ECOM+BW	4.1	4.8	3.7	10.5
ECOM2	6.0	8.2	14.1	28.2
ECOM2+BW	11.4	7.4	6.0	19.3

Mean offsets and STDs of SLR residuals are given in Table 7. The pure ECOM2 model reduces the STD of SLR residuals by about 60% over the pure ECOM model in YS mode while about 20% in ON mode. Combined with the a priori box-wing model the ECOM2 model marks further improvement of about 10% and 30% over the pure ECOM2 model in YS and ON mode respectively. The ECOM+BW model provides the best QZS-1 orbits, a clear improvement of 40% and 60% can be observed in SLR residuals over the pure ECOM2 model in YS and ON mode respectively. Moreover, the mean offset of the SLR residuals reduces from more than 20 cm for the ECOM model to as good as 4 cm in the ECOM+BW model.

Obviously, QZS-1 orbits benefit more from the a priori box-wing model than Galileo orbits, and BeiDou-2 orbits almost show no change. The reason is that Galileo and QZS-1 are stretched body satellites and the latter has much larger dimensions. SRP acceleration varies periodically due to the asymmetric body dimensions, which cannot be modeled very well by the ECOM model. The additional higher order Fourier series in the ECOM2 model compensate such periodical SRP accelerations better than the ECOM model. However, deficiencies of the ECOM2 model are identified in ON mode for QZS-1 orbits, and the use of a priori box-wing model can compensate such disadvantages fairly well.

5. Initial Results of BeiDou-3e and QZS-2

Zhao et al. (2018b) remarked that BeiDou-3e satellites did not use ON mode but experience midnight and noon maneuvers when $|\beta| < 3°$. In November 2017 the NSPCJ published the attitude mode as well as the dimensions of QZS-2 satellite. It operates always in YS mode except for the period in which the orbit control maneuver is conducted. So, in our study, only YS related optical parameters are adjusted for BeiDou-3e and QZS-2 satellites. The approximate dimensions of the BeiDou-3e I2S satellite (Wang et al., 2018) are assumed to be the same for all the BeiDou-3e satellites. In the MGEX network, there are around 20 stations tracking the QZS-2 and BeiDou-3e satellites. The time period used starts from 2017 day 330 to 2018 day 90, and the processing standards are the same as shown in section 3.

Table 8 exhibits the adjusted optical properties of BeiDou-3e and QZS-2 satellites. The sum of $\alpha + \delta$ and ρ for BeiDou-3e satellites deviate more from 1 than for the QZS-2 satellite, which might be due to the errors in the assumed dimensions. With the adjusted parameters, we test the four types of SRP models for QZS-2 and BeiDou-3e satellites as well. Figure 8 illustrates the SLR residuals of QZS-2 orbits. We observe immediately that the ECOM2 and ECOM2+BW orbits show large scattered SLR residuals during the eclipsing season while the ECOM+BW orbits do not vary much. Mean offsets and STDs of SLR residuals are given in Table 9. The pure ECOM2 model reduces the STD of SLR residuals by about 30% over the pure ECOM model for the non-eclipsing period, while an increase of about 40% is observed during the eclipsing season. The ECOM+BW SRP model results in the best QZS-2 orbits both in eclipsing and non-eclipsing seasons, and marks an overall improvement of about 30% over the other

Table 8: The estimated optical metadata and formal errors for BeiDou-3 and QZS-2 satellites

BeiDou-3e	$A(m^2)$	$\alpha+\delta$	ρ	QZS-2	$A(m^2)$	$\alpha+\delta$	ρ
+x	7.200	0.064±0.015	0.211±0.015	+x	14.880	0.911±0.013	0.011±0.005
+z	5.000	0.386±0.013	0.403±0.015	+z	5.760	1.084±0.026	0.283±0.010
−z	5.000	0.971±0.013	-0.424±0.016	−z	5.760	0.496±0.027	1.217±0.025

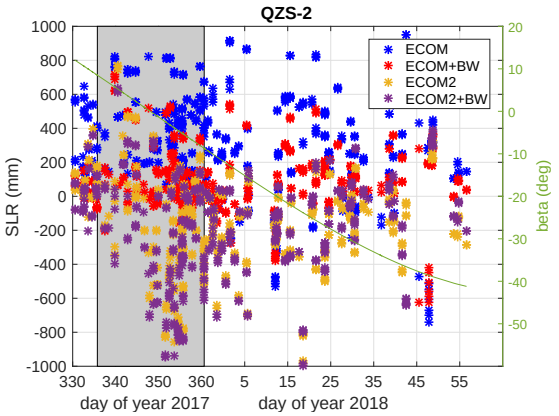

Figure 8: SLR residuals of QZS-2 orbits. (blue: pure ECOM, red: ECOM+BW, yellow: pure ECOM2, purple: ECOM2+BW). The β angle is indicated by a solid green line and the eclipsing seasons are indicated in grey.

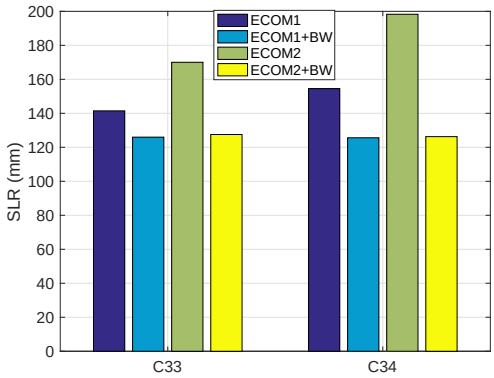

Figure 9: STDs of SLR residuals for BeiDou-3e orbits.

Table 9: Mean offset and STD of SLR residuals for QZS-2 orbits. unit (cm)

	Non-eclipsing	Eclipsing
ECOM	26.9±31.7	39.3±22.4
ECOM+BW	7.9±19.9	13.1±18.2
ECOM2	-14.7±23.4	-17.4±34.9
ECOM2+BW	-14.1±25.7	-25.1±35.1

SRP models. Moreover, the mean offset of SLR residuals is significantly reduced by a factor of 3 times over orbit products derived by the pure ECOM model. In fact, by the end of our work, we find that the QZS-2 satellite providers has recently published their optical properties (http://qzss.go.jp). To evaluate our adjustments, we introduce the officially published parameters into the a priori box-wing model and validate the orbit estimations. Results prove that the STD of SLR residuals is about 2 cm smaller than by using our estimated optical parameters. Thus, even if provided with a small network our estimation procedure can still achieve comparable results with the published parameters.

SLR observations of BeiDou-3e satellites were only available for C33 and C34 satellites during the experimental periods, the STDs of SLR residuals are shown in Figure 9. The ECOM2 model demonstrates larger STDs than the ECOM model. The ECOM+BW SRP model presents the smallest STD of about 13 cm for BeiDou-3e orbits, which indicates an improvement of about 20% over orbit products without the a priori box-wing model. Moreover, the EOCM2 model benefits also from the a priori box-wing model and results in almost the same STD as the ECOM+BW model.

6. Summary and conclusion

A precise box-wing model depends highly on the metadata and attitude of a satellite. In this study, satellite attitudes are taken from the information provided by the system operators, areas and masses of satellites are fixed to the published or guessed values, and the optical properties are estimated. The adjusted results show that our estimation procedure reproduces the published parameters fairly well for Galileo satellites, but differences between estimated corrections and the initial values are identified for BDS and QZS-1 satellites. Validation from orbit prediction proves that the adjusted parameters of Galileo and QZS-1 satellites show almost the same performance as the corresponding published or "best guess" values, whereas, a large improvement over 60% is pointed out for BDS satellites by using the adjusted parameters.

With the resulting metadata, we aim to set up an optimal SRP model for individual constellations. Orbit validation from SLR residuals demonstrates that the pure ECOM2 model performs better than the pure ECOM model for Galileo, BDS GEO and QZS-1 orbits, but there is no large difference for BDS IGSO and MEO orbits. When combining with an a priori box-wing model, the ECOM model benefits more than the ECOM2 model and results in the best Galileo, BDS GEO and QZS-1 orbits. STD of SLR residuals reduces further by about 20% and

5% over the pure ECOM2 model for Galileo and BDS GEO orbits, while the reductions are about 40% and 60% for QZS-1 orbits in yaw-steering and orbit-normal mode respectively. However, BDS IGSO and MEO satellite orbits do not benefit much from the a priori box-wing model even if provided with the adjusted metadata. In summary, we suggest setting up a unified SRP model of ECOM+BW for Galileo, QZS-1, and BDS GEO satellite orbit determination based on the adjusted metadata.

Finally, we adjust the optical properties of BeiDou-3e and QZS-2 satellites using a limited number of tracking stations. SLR validation of orbits proves that the ECOM2 model performs better than the ECOM model for QZS-2 orbits during the non-eclipsing season, but degradation is found during the eclipsing season. For BeiDou-3e orbits, the pure ECOM model show better performance than the pure ECOM2 model. Combined with the a priori box-wing model the ECOM model results in the best QZS-2 and BeiDou-3e orbits, an improvement of about 30% and 20% is observed respectively compared to orbits without an a priori model. Moreover, the latest published optical parameters of QZS-2 satellite verifies that our estimation procedure can achieve comparable results even if provided with a limited network. It is easy to apply to the new emerging satellites in the future.

Acknowledgments

This research is based on the analysis of Multi-GNSS observations provided by the IGS MGEX. The effort of all the agencies and organizations as well as all the data centers is acknowledged. Satellite laser ranging observations of Galileo, BeiDou-2, BeiDou-3, QZS-1, QZS-2 are taken from cddis.gsfc.nasa.gov, which are essential for orbit validation. We would like to thank the International Satellite Laser Ranging Service (ILRS) as well as the effort of all respective station operators.

References

Arnold, D., Meindl, M., Beutler, G., Dach, R., Schaer, S., Lutz, S., Prange, L., Sośnica, K., Mervart, L., Jäggi, A., 2015. CODE's new solar radiation pressure model for GNSS orbit determination. Journal of geodesy 89, 775–791.

Beutler, G., Brockmann, E., Gurtner, W., Hugentobler, U., Mervart, L., Rothacher, M., Verdun, A., 1994. Extended orbit modeling techniques at the CODE processing center of the international GPS service for geodynamics (IGS): theory and initial results. Manuscr. Geod. 19, 367–386.

Beutler, G., Brockmann, E., Hugentobler, U., Mervart, L., Rothacher, M., Weber, R., 1996. Combining consecutive short arcs into long arcs for precise and efficient GPS orbit determination. Journal of Geodesy 70, 287–299.

Dach, R., Hugentobler, U., Fridez, P., Meindl, M., et al., 2007. Bernese GPS software version 5.0. Astronomical Institute, University of Bern .

Dai, X., Ge, M., Lou, Y., Shi, C., Wickert, J., Schuh, H., 2015. Estimating the yaw-attitude of BDS IGSO and MEO satellites. Journal of Geodesy 89, 1005–1018.

Deng, Z., Fritsche, M., Uhlemann, M., Wickert, J., Schuh, H., 2016. Reprocessing of GFZ multi-GNSS product GBM, in: Proceedings of IGS Workshop, Sydney Australia.

Fliegel, H., Gallini, T., Swift, E., 1992. Global positioning system radiation force model for geodetic applications. Journal of Geophysical Research: Solid Earth 97, 559–568.

Fliegel, H.F., Gallini, T.E., 1996. Solar force modeling of block IIR global positioning system satellites. Journal of Spacecraft and Rockets 33, 863–866.

Guo, J., Chen, G., Zhao, Q., Liu, J., Liu, X., 2017. Comparison of solar radiation pressure models for BDS IGSO and MEO satellites with emphasis on improving orbit quality. GPS Solutions 21, 511–522.

Guo, J., Xu, X., Zhao, Q., Liu, J., 2016. Precise orbit determination for Quad-constellation satellites at Wuhan University: strategy, result validation, and comparison. Journal of Geodesy 90, 143–159.

Inaba, N., Matsumoto, A., Hase, H., Kogure, S., Sawabe, M., Terada, K., 2009. Design concept of quasi zenith satellite system. Acta Astronautica 65, 1068–1075.

Ishijima, Y., Inaba, N., Matsumoto, A., Terada, K., Yonechi, H., Ebisutani, H., Ukawa, S., Okamoto, T., 2009. Design and development of the first Quasi-Zenith satellite attitude and orbit control system, in: Aerospace conference, 2009 IEEE, IEEE. pp. 1–8.

Li, X., Ge, M., Dai, X., Ren, X., Fritsche, M., Wickert, J., Schuh, H., 2015. Accuracy and reliability of Multi-GNSS real-time precise positioning: GPS, GLONASS, BeiDou, and Galileo. Journal of Geodesy 89, 607–635.

Milani, A., Nobili, A.M., Farinella, P., 1987. Non-gravitational perturbations and satellite geodesy. Adam Hilger, Bristol, UK .

Montenbruck, O., Schmid, R., Mercier, F., Steigenberger, P., Noll, C., Fatkulin, R., Kogure, S., Ganeshan, A.S., 2015a. GNSS satellite geometry and attitude models. Advances in Space Research 56, 1015–1029.

Montenbruck, O., Steigenberger, P., Darugna, F., 2017a. Semi-analytical solar radiation pressure modeling for QZS-1 orbit-normal and yaw-steering attitude. Advances in Space Research 59, 2088–2100.

Montenbruck, O., Steigenberger, P., Hugentobler, U., 2015b. Enhanced solar radiation pressure modeling for Galileo satellites. Journal of Geodesy 89, 283–297.

Montenbruck, O., Steigenberger, P., Prange, L., Deng, Z., Zhao, Q., Perosanz, F., Romero, I., Noll, C., Stürze, A., Weber, G., et al., 2017b. The Multi-GNSS experiment (MGEX) of the International GNSS Service (IGS)–achievements, prospects and challenges. Advances in space research 59, 1671–1697.

Pearlman, M.R., Degnan, J.J., Bosworth, J.M., 2002. The international laser ranging service. Advances in Space Research 30, 135–143.

Prange, L., Orliac, E., Dach, R., Arnold, D., Beutler, G., Schaer, S., Jäggi, A., 2017. CODE's five-system orbit and clock solution - the challenges of multi-GNSS data analysis. Journal of geodesy 91, 345–360.

Rodriguez-Solano, C., Hugentobler, U., Steigenberger, P., 2012a. Adjustable box-wing model for solar radiation pressure impacting GPS satellites. Advances in Space Research 49, 1113–1128.

Rodriguez-Solano, C., Hugentobler, U., Steigenberger, P., Lutz, S., 2012b. Impact of Earth radiation pressure on GPS position estimates. Journal of geodesy 86, 309–317.

Selmke, I., Hugentobler, U., 2017. Multi-GNSS orbit determination using 2-step PPP approach, in: Proceedings of IGS Workshop, Paris, France.

Steigenberger, P., Hauschild, A., Montenbruck, O., Rodriguez-Solano, C., Hugentobler, U., 2013. Orbit and clock determination of QZS-1 based on the CONGO network. Navigation 60, 31–40.

Steigenberger, P., Hugentobler, U., Loyer, S., Perosanz, F., Prange, L., Dach, R., Uhlemann, M., Gendt, G., Montenbruck, O., 2015a. Galileo orbit and clock quality of the IGS Multi-GNSS Experiment. Advances in space research 55, 269–281.

Steigenberger, P., Montenbruck, O., Hugentobler, U., 2015b.

GIOVE-B solar radiation pressure modeling for precise orbit determination. Advances in Space Research 55, 1422–1431.

Wang, C., Guo, J., Zhao, Q., Liu, J., 2018. Solar radiation pressure models for BeiDou-3 I2-S satellite: Comparison and augmentation. Remote Sensing 10, 118.

Zhao, Q., Chen, G., Guo, J., Liu, J., Liu, X., 2018a. An a priori solar radiation pressure model for the QZSS Michibiki satellite. Journal of Geodesy 92, 109–121.

Zhao, Q., Wang, C., Guo, J., Wang, B., Liu, J., 2018b. Precise orbit and clock determination for BeiDou-3 experimental satellites with yaw attitude analysis. GPS Solutions 22, 4.